Adsorption Behavior of Radionuclides, ^{137}Cs and ^{140}Ba, onto Solid Humic Acid

O. Çelebi and H.N. Erten

Abstract In this research, the adsorption behaviors of two important fission product radionuclides (^{137}Cs and ^{133}Ba) onto sodium form of insolubilized humic acid (INaA) were investigated as a function of time, cation concentration and temperature, utilizing radiotracer method. The resulting data was fitted well to the Freundlich and Dubinin-Radushkevich (D-R) isotherms. Thermodynamic constants such as; free energy (ΔG_{ads}), enthalpy (ΔH_{ads}), entropy (ΔS_{ads}) of adsorption were determined. Temperature change didn't effect sorption processes significantly. Best fitting kinetic models were found for a better understanding of adsorption mechanisms. It was found that Ba^{2+} was adsorbed five times more than Cs^{+} onto structurally modified humic acid and kinetic studies indicated that adsorption behaviors of both ions obey the pseudo second order rate law. The effect of pH changes on adsorption was also examined and optimum pH range was found in the range of pH 6–8. FTIR and solid state carbon nmr (^{13}CNMR) spectroscopic techniques were used to understand the structural changes during insolubilization process. Quantitative determination of adsorption sites was carried out using potentiometric titration method and the resulting data was treated by using appropriate Gran functions.

Keywords Adsorption · Isotherm models · IHA · Thermodynamic constants · Kinetic studies · Distribution ratio · HA · INaA · Radiotracer method · Radionuclide · Batch method · Spectroscopy · pH

1 Introduction

There is an increasing effort for removing highly soluble radiocontaminants from aqueous waste streams by fixing them onto solid waste forms that can be disposed of in a repository. In this way, the high-volume aqueous streams are transformed

O. Çelebi (✉)
Department of Chemistry, Bilkent University, 06800 Bilkent Ankara, Turkey
e-mail: celebi@fen.bilkent.edu.tr

H. Gökçekuş et al. (eds.), *Survival and Sustainability*, Environmental Earth Sciences,
DOI 10.1007/978-3-540-95991-5_101,

from a high-level radioactive waste into a low-level radioactive waste that is much cheaper to treat. However, the removal of this species may not only serve environmental initiatives, but it may also serve as a means of producing useful materials for use in science and industry. It is known, for example, that ^{137}Cs is an excellent γ source for medical applications such as instrument disinfection and radiotherapy. Similarly, ^{137}Cs has also proven to be useful as source for sterilization in the food industry. The radionuclide ^{137}Cs is produced in high yield during the fission process and due to its long half-life ($T_{1/2} = 30.17$ years) and its high solubility in aqueous media, it is a principal radiocontaminant in radioactive wastes [1, 2].

Barium is an alkaline earth element ($Z = 56$), its radioactive isotope ^{140}Ba ($T_{1/2} =$ 12.79 day) is a fission product with a high yield (6.21%). This radionuclide is a serious radiocontaminant, furthermore being a homologue of Ra, Ba^{2+} is a suitable cation for the radiochemical study of Ra^{2+}, which have several radioisotopes that are important in radioactive waste considerations. $^{133}Ba^{2+}$ was chosen as a radiotracer in our studies because of its long half-life ($T_{1/2} = 10.7$ years) and a γ-ray at 356 keV energy [3].

Humic substances (HS) are the most abundant reservoir of carbon on earth. Humic acids (HAs) are operationally defined as the fraction of HS that is insoluble in water at low pH(<2) and soluble at higher pH (>2). HAs perform various roles in soil chemistry. They act as soil stabilizers, nutrient and water reservoirs for plants, sorbents for toxic metal ions, radionuclides and organic pollutants, stimulate plant growth, and biotransform toxic pollutants. When leached into surface waters, they also play a pivotal role in the aquatic environment. For example, they bind and transport metal ions. In earlier studies it was classified as a natural or biopolymer which is not a well-defined molecular species, polydisperse (composed of many molecular weights [MWs]), irregular in structure, and varies in elemental composition with its natural origin [4, 5]. However, recent information gathered using spectroscopic, microscopic, pyrolysis, and soft ionization techniques is not consistent with the “polymer model” of humic substances. A new concept of humic substances has thus emerged, that of the supramolecular association, in which many relatively small and chemically diverse organic molecules form clusters linked by hydrogen bonds and hydrophobic interactions. A corollary to this model is the concept of micellar structure, i.e., an arrangement of organic molecules in aqueous solution to form hydrophilic exterior regions shielding hydrophobic interiors from contact with vicinal water molecules [6].

Generally, humic acid is soluble above pH 3 in aqueous media and this makes humic acid an inappropriate sorbent for traditional operations such as adsorption and recovery of metal ions in aqueous media. The solubility of humic acid in aqueous media depends on the number of $-COOH$ and $-OH$ groups present on humic acid on a large scale and with increasing content of these groups solubility increases. These groups also give humic acid the ability to interact with metal ions through adsorption, ion-exchange, and complexation mechanisms. However, the high solubility of humic acid in aqueous media is a limiting problem for taking advantage of the interaction ability of humic acid (as a solid phase) with metal ions. Accordingly, it is not advisable to use untreated humic acid as a sorbent in aqueous media, so an appropriate treatment of humic acid is needed [7].

The process developed by Seki and Suzuki [8] is called "insolubilization of humic acid" and with this method humic acid can be converted to a form which is insoluble up to pH 10 in aqueous media.

To properly understand an adsorption process, we must understand two basic phenomena: equilibrium and kinetics. With regards to adsorption processes, thermodynamic data only provide information about final state of a system, but kinetics deals with changes in chemical properties in time and is concerned especially with rates of changes. Adsorption kinetics is of interest for many aspects of surface chemistry, from understanding of adsorption mechanisms to more practical problems such as removal of pollutant components from solutions [9].

In this research, the adsorption behaviors of the fission product radionuclides ^{137}Cs and ^{133}Ba onto insolubilized humic acid were investigated both thermodynamically and kinetically and resulting data was analyzed by using Freundlich and Dubinin-Radushkevich (D-R) isotherms. The structural changes during insolubilization process were determined by spectroscopic techniques and also quantitative determination of adsorption sites was carried out.

A number of articles have been published in the field of adsorption of cations onto insolubilized humic acid. Gezici et al. [7] reported the sorption behavior of a nickel-insolubilized humic acid system in a column arrangement. In another study Baker and Khalili [10] published the analysis of the removal of lead(II) from aqueous solutions by adsorption onto insolubilized humic acid. El-Eswed and Khalili [11] reported the adsorption of Cu(II) and Ni(II) on solid humic acid.

However, no published report on the study of the adsorption behavior of cations onto insolubilized humic acid using radiotracers was found in our literature. This study is a chemical approach in the study of the adsorption behavior of radiocontaminants onto natural materials and also shows the use of solid humic acid as a good adsorbent for the sorption of radionuclides.

2 Mathematical Relations

2.1 The Distribution Ratio

The experimental data in adsorption are expressed in terms of the ditribution ratio, R_d, defined as the ratio of adsorbate concentration on solid phase to its concentration in liquid phase. The distribution ratio of adsorption is defined as:

$$R_\mathrm{d} = \frac{[\mathrm{C}]_s}{[\mathrm{C}]_l} \tag{1}$$

where $[\mathrm{C}]_s$ (mmol/g) and $[\mathrm{C}]_l$ (mmol/ml) are the concentrations of species C in the solid and liquid phases, respectively. At the beginning of the sorption step, V (ml) of solution with initial concentration $[\mathrm{C}]^\circ$ (mmol/ml) is used and at the end of the sorption step V (ml) of solution with concentration $[\mathrm{C}]_l$ are present, hence the concentration of C in the solid phase after sorption can be expressed as:

$$[\mathrm{C}]_s = \frac{V([\mathrm{C}]^\circ - [\mathrm{C}]_l)}{W_s} \tag{2}$$

In terms of radiactivity, $[\mathrm{C}]_l$ can be written as:

$$[C]_l = \frac{A_l}{A^\circ}[C]^\circ \tag{3}$$

From Eqs. (1), (2), and (3), the following equation is obtained:

$$R_\mathrm{d} = \frac{VA^\circ - VA_l}{A_l W_s} \tag{4}$$

where A° is the initial count rate of solution added for sorption (cps)/ml, A_l is the count rate of solution after sorption (cps)/ml, W_s is the weight of solid material (g) [12].

2.2 Adsorption Isotherms

An isotherm describes the relationship of the concentrations of a solute between two separate phases at equilibrium at a constant temperature. An adsorption isotherm, then would express the relation between the amount of solute or vapor adsorbed as a function of the equilibrium concentration of the solute or vapor in solution. A sorption isotherm describes the process without reference to the mechanism [13].

2.2.1 Freundlich Isotherm[3]

Freundlich isoterm model is one of the most used non-linear model for describing the dependence of sorption on sorbate concentration. This model allows for several kinds of sorption sites on solid and represents properly the sorption data at low and intermediate concentrations on heterogeneous surfaces. The general expression of Freundlich isotherm is given as:

$$[\mathrm{C}]_s = k[\mathrm{C}]_l^n \tag{5}$$

Where $[\mathrm{C}]_s$ is the amount of ionic species adsorbed on the solid matrix at equilibrium (mmol/g), $[\mathrm{C}]_l$ is the concentration of the cation in solution at equilibrium (mmol/ml), k and n are Freundlich constants.

This expression can be linearized as:

$$\log\,[\mathrm{C}]_s = \log\,k + n\,\log\,[\mathrm{C}]_l \tag{6}$$

Plotting $\log\,[\mathrm{C}]_s$ versus $\log\,[\mathrm{C}]_l$ yields n as the slope and $\log k$ as the intercept.

2.2.2 Dubinin Raduskevich (D-R) Isotherm[3]

The D-R isotherm model is valid at low concetration ranges and can be used to describe sorption on both homogeneous and heterogeneous surfaces. It can be represented by the general expression:

$$[\mathrm{C}]_s = [\mathrm{C}]_m \exp -(K\varepsilon^2) \tag{7}$$

where $[\mathrm{C}]_s$ and $[\mathrm{C}]_l$ are as defined above, ε is the polanyi potential, given as RT ln(1+1/$[\mathrm{C}]_l$), R is the ideal gas constant (8.3145 J/mol.K), T is the absolute temperature(K), K is a constant related to the energy of sorption and C_m is the sorption capacity of adsorbent per unit weight (mmol/g).

The linear form of the equation above can be obtained by rearranging it to give:

$$\ln\,[\mathrm{C}]_s = \ln\,[\mathrm{C}]_m - K\varepsilon^2 \tag{8}$$

If ln $[\mathrm{C}]_s$ is plotted against ε^2, K and lnC_m will be obtained from the slope and the intercept, respectively. The value of K (mol/kJ)^2 is related to the adsorption mean free energy, E (kJ/mol), defined as the free energy change required to transfer one mole of ions from infinity in solution to the solid surface. The relation is given as:

$$E = (2\,K)^{-1/2} \tag{9}$$

3 Experimental

3.1 Chemicals

All used chemicals were of analar grade. Humic acid sample was taken from Ankara university, Agricultural Faculty, Soil Science department.

3.2 Isolation and Insolubilization of Humic Acid

Humic acid was isolated from a partially purified soil (contains 55% humic acid, 30% fulvic acid, %12 K_2O) by the following procedure; Stirring crude humic acid in 1% NaOH solution for 1 h and subsequent centrifugation at 5,000 rpm, dissolved fraction was taken and adjusted pH 2 with HCl, stirred for 4 h and subsequent centrifugation at 5,000 rpm. Resulting precipitate was taken and repeated this procedure two more times. The precipitate was rinsed with deionized water many times to remove chloride ions. After dechlorination step, HA was dried at 95°C for 4 h.

Humic acid was insolubilized by heating in a temperature controlled oven at 330°C for 1.5 h and solid phase (IHA) was converted to its sodium form (INaA) by stirring IHA in a 1 M $NaNO_3$ solution for 2 days, resulting solid phase was dried at 80°C.

3.3 Quantitative Determination of Adsorption Sites on HA

Adsorption sites (carboxylic and phenolic groups) were determined quantitatively by using potentiometric titration method. Model 5669-20 pH meter, Cole Parmer Instrument Company, was used for pH measurements. Titration was carried out from pH 3.5 to 10.58 using 0.1 M NaOH as titrant. Analyte was containing 50 ml suspension of humic acid (576 mg l^{-1}). This value was also used by other studies[14]. Nitrogen gas was passed through the solution until titration finished to prevent CO_2 interference. Resulting data was linearized by using the appropriate Gran functions [15]. Total acidity value was supposed to the total of carboxlic and phenolic acidities.

3.4 Adsorption Experiments

3.4.1 Radiotracer Method

Batch method was applied throughout the study. The tracers used in sorption experiments were ^{137}Cs ($T_{1/2} = 30.17$ years) and ^{133}Ba ($T_{1/2} = 10.7$ years). 1 L of stable isotope solutions were spiked with few microliters (∼400 μL) of the corresponding radionuclide solutions used in different experiments. The initial count rates were measured for 2.5 ml aliquots of cesium and barium solutions using the prominent γ rays of 662 and 361 keV, respectively. Initial acitivity was adjusted not to be lower value than 10,000 (cps)/ml.

A NaI(Tl) detector detector was used during radioactivity measurements of samples. All the experiments were performed in duplicates. In order to check any loss in activity originating from adsorption on the inside wall of tubes, blank experiments were performed using solutions without adsorbent. The results showed that adsorption onto the tube walls was negligible.

3.4.2 Kinetic Studies

To each of a set of INaA samples placed in tubes, 7.5 ml of Cs^+ solution (prepared from CsCl salt) containing an appropriate amount of ^{137}Cs radiotracer was added. The initial concentration of solution was 1×10^{-4} M. Samples were shaken at room temperature for periods ranging from 5 min to 48 h. They were centrifuged and 2.5 ml portions of the liquid phases were counted to determine their activities. The same procedure was applied for barium sorption studies using 9 ml of Ba^{2+} solution (prepared from $BaCl_2$ salt) having an appropriate amount of ^{133}Ba radiotracer.

3.4.3 Effect of Loading, Temperature and pH

Loading experiments were carried out to investigate the effect of initial cation concentrations on sorption at four different temperatures; 15, 25, 35, 45°C and at the initial concetrations of 5×10^{-4}, 1×10^{-4}, 1×10^{-5}, 5×10^{-6} (mmol/ml) for Cs^+

sorption. In the case of Ba^{2+} sorption the maximum temperature was 55°C and concentrations used were 1×10^{-4}, 1×10^{-5}, 5×10^{-6}, 1×10^{-6} (mmol/ml). Samples were prepared as in the case of kinetic experiment, but all concentrations were used instead of only 1×10^{-4} M. The effect of pH upon sorption behavior of Ba^{2+} onto INaA was investigated at a fixed concentration (1×10^{-5}) and room temperature with varying pH values ranging from 1.5 to 10. The samples were shaken for 1 day, centrifuged and 2.5 ml of portions of the liquid phase were counted. Shaking was done in a temperature controlled environment using a Nuve ST 402 water bath shaker equipped with microprocessor thermostat. The fluctuation in controlled temperature was ± 1°C.

3.5 Spectroscopic Characterization of Humic Acid and Insolubilized Humic Acid

3.5.1 FTIR

FT-IR spectra were recorded using a Bruker Tensor 27 FTIR spectrometer with a standard high sensitivity DLATGS detector, with a resolution of 4 cm^{-1} and 64 scans, The KBr pellets were obtained by pressing a mixture of 1:100 ratio of humic acid samples and KBr, respectively.

3.5.2 ^{13}C CP/MAS NMR

Solid-state ^{13}C NMR spectra were obtained at the ^{13}C resonance frequency of 125.721 MHz on a Bruker Avance ASX 500 spectrometer, equipped with a double resonance HX probe. The samples were confined in a zirconium oxide rotor with an external diameter of 2.5 mm. The Cross-Polarization Magic Angle Spinning CPMAS technique was applied with a contact time of 1 ms, a spinning speed of 15 kHz MAS and a pulse delay of 2s.

4 Results and Discussion

4.1 Potentiometric Titration

To quantify the acidic functional (carboxylic and phenolic) groups, potentiometric titration method was used. It is usual to plot the differential curves, $\Delta pH/\Delta V$ or $\Delta E/\Delta V$ against volume of titrant added, but when the titration curve is not symmetrical about the equivalence point, as in Fig. 1, then it is possible to obtain erroneous results. Therefore, G. Gran [15] developed mathematical expressions to linearize various titration curves. In our data treatment, we chose the following equation, assuming humic acid as a polymeric acid and titration type as weak acid-strong base titration Fig. 2.

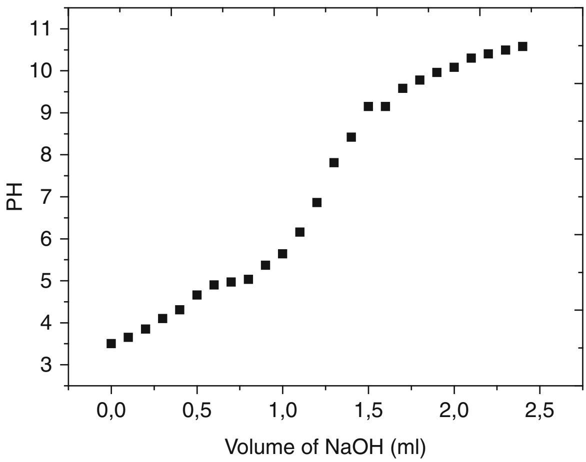

Fig. 1 Potentiometric titration curve of HA

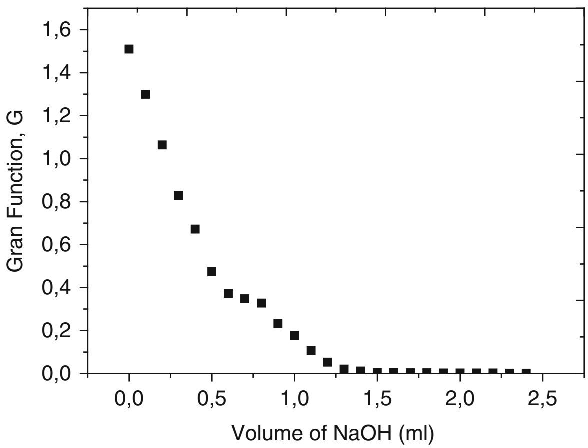

Fig. 2 Linearized plot potentiometric titration curve of HA

$$G = V \times 10^{\mathrm{pH}-k} \tag{10}$$

where V represents the amount of titrant used (ml) and k is an arbitrary constant with a value such that the antilogarithms will fall in a suitable range such as 0 to 100–1,000.

After conversion of the potentiometric titration data to linearized form Fig. 2 using Gran functions, two associated linear curves were obtained. The following quantitative acidic functional group and total acidity values are given in Table 1.

Table 1 Acidic functional group contents obtained experimentally using potentiometric titration (meq/100 g) of humic acid

HA	-COOH	$-C_6H_5OH$	Total acidity
	249.0	190.0	439.0

4.2 FTIR and ^{13}C NMR Spectra of HA and INaA

FTIR spectroscopic technique was used to examine the structural changes after insolubilization process. The peaks and corresponding functional groups in FTIR spectrum shown in Fig. 3 are as follows; a broad band at 3,387 cm^{-1} primarily corresponds to O-H stretching and secondarily to N-H stretching, the peak at 3,071 cm^{-1} represents stretching of aromatic C-H, absorption bands at 2,928 and 2,857 cm^{-1} are attributed to aliphatic C-H stretching in CH_2 and CH_3, respectively, Broad bands at 2,500 cm^{-1} is overtone from carboxylic groups stretching ($2 \times$ 1,246 cm^{-1}) and at 2,000 cm^{-1} is overtone from C-O polysaccharides stretching mode ($2 \times$ 1,060 cm^{-1}), Strong absorption band at 1,704 cm^{-1} is due to C=O stretching of carboxylic acid and ketone and absorption bands at 1,602 cm^{-1} and 1,372 cm^{-1} are ascribed to stretching of carboxylate ion and the peak at 1,602 cm^{-1} can also be attributed to structural vibrations of aromatic C=C bonds, the peak at 1,222 cm^{-1} represents C-O stretching in phenols and O-H deformation of COOH. The absorptions from deformation of aliphatic C-H and, H-bonded C=O of conjugated ketones and water deformation occurs at 1,448 cm^{-1}, the band at 1,033 cm^{-1} represents C-O stretching of polysaccharides. [16, 17, 18].

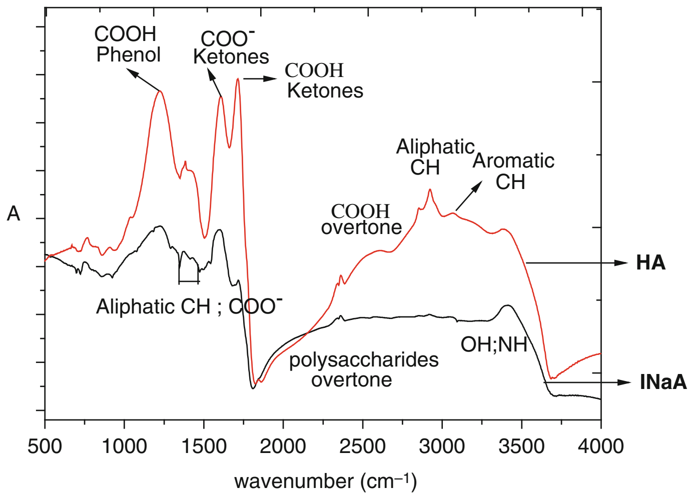

Fig. 3 FTIR spectra of HA and INaA

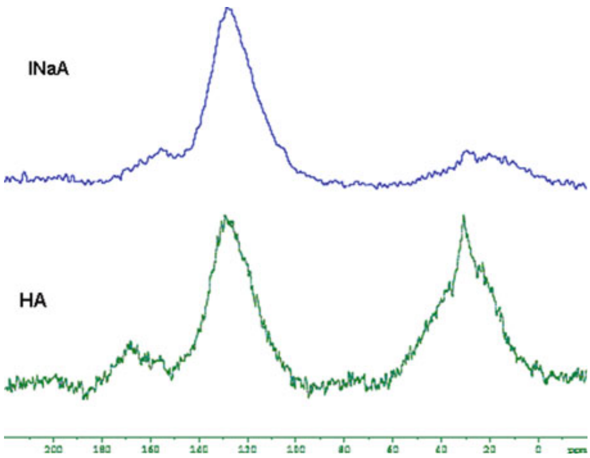

Fig. 4 ^{13}C NMR spectra of HA and INaA

The ^{13}C spectra in Fig. 4 of HA and INaA include following peaks: (a) alkyl carbons and *O*-alkyl carbons (aminoacids/carbons adjacent to ester/ether/hydroxyl) (0–60 ppm), because that peak was not well resolved we observe those two groups in a broad band; (110–145) ppm is assigned to aromatic carbon, the at (150–190) ppm include phenolic and carboxylic carbons [19, 20, 21].

When we examine FTIR and ^{13}C NMR spectra of HA and INaA, we observe that there is a decrease at the intensities of aliphatic alkyl groups, -COOH group and phenolic groups, the effect causing insolubilization is mainly due to loss in carboxyl groups, but as we see on spectrum, all of the adsorption sites are not lost during insolubilization. In literature [8] it was found by titration methods that the lost in percentage of acidic functional groups is nearly 25%. By this way, the ability of HA to make hydrogen bonding decreased and that caused the insolubilization of HA in water at high pH values.

It is also clear from the ^{13}C NMR that aromatic part of HA is not affected after insolubilization, because there is no intensity change.

4.3 Kinetic Studies

The sorption studies of Cs^{+} and Ba^{2+} ions on INaA as a function of time were performed for time intervals ranging from 5 min up to 48 h. Plots of the variation of R_d as a function of time for Cs^{+} and Ba^{2+} ions are given in Figs. 5 and 6, respectively.

It is apparent that, equlibrium is reached after several hours of contact. Such a rapid process indicates that sorption is primarily a surface phenomena where the humic acid surface is readily accessible to ions in solution. On the basis of the obtained results an equilibrium period of 1 day was selected as a fixed parameter for further experiments, where the effects of loading and temperature, were examined.

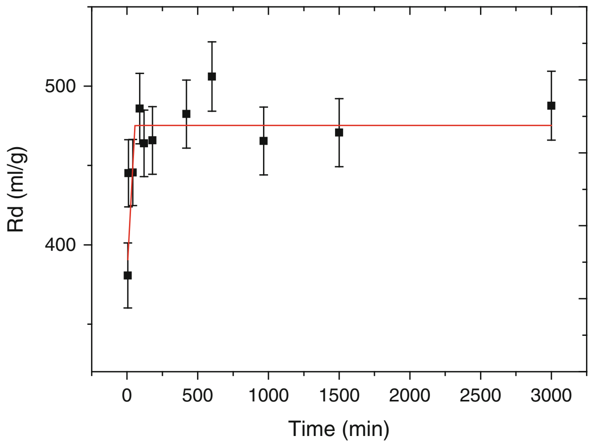

Fig. 5 Variation of R_d values with shaking time for Cs^+ sorption on INaA at 25°C

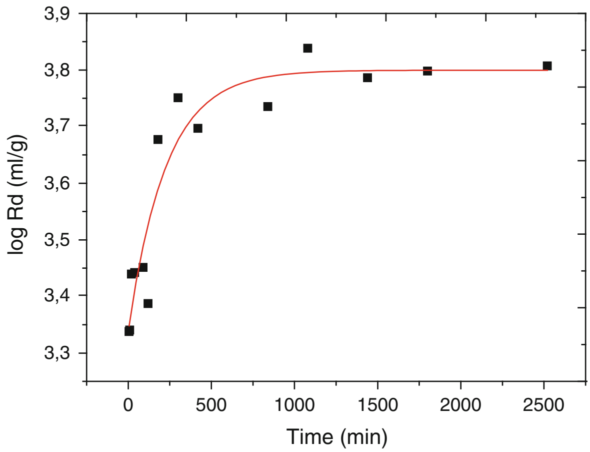

Fig. 6 Variation of log R_d values with shaking time for Ba^{2+} sorption on INaA at 25°C

Kinetic studies were also used to determine best fitting rate equations and rate constants of cation sorption. S. Azizian [9] has published kinetic models for the sorption behavior of solutes onto adsorbent and in his research it has been shown that at lower initial concentration of solute, the mechanism obeys pseudo second order model. The rate law for this system is expressed as:

$$\frac{dq}{dt} = k_2(qe - q)^2 \tag{11}$$

where q and q_e are the amount of solute sorbed per gram of sorbent at any time and at equilibrium, respectively, and k_2 is the pseudo second order rate constant of sorption. After integration and rearrangement of the above equation, the following equation is obtained with a linear form,

Table 2 Amount of sorbed cation per gram of sorbent, pseudo second order rate constants and correlation coefficient values for cesium and barium sorption

Sorbed cations	q_e (mol/g)	k_2 (g.mol^{-1}. min^{-1})	R^2
Cs^+	29.44×10^{-3}	9.998	0.9998
Ba^{2+}	141.30×10^{-3}	0.432	0.9997

$$\frac{t}{q} = \frac{1}{k2q_e^2} + \frac{1}{q_e}t \tag{12}$$

The plot of t/q versus t gives a straigt line with slope of $1/k_2q_e^2$ and intercept of $1/q_e$. So the amount of cation sorbed per gram of sorbent (INaA) at equilibrium q_e and sorption rate constant k_2 could be evaluated from the slope and intercept, respectively. The results obtained are shown in Table 2.

It is apparent from q_e values that barium ions are sorbed five times more than cesium ions and rate constant values show that cesium much more rapidly adsorbed by INaA, rate constant value of cesium sorption is obviously greater than barium sorption. Correlation coefficient values indicate that pseudo second order rate equation almost completely fit for sorption behavior of low concentration of cesium and barium ions onto INaA.

The reason for the less sorption tendency of cesium ions onto INaA can be explained by their charge. An increase in the oxidation state favors the accumulation of the ions on the sorption surface leading to electrostatic stability.

4.4 Loading Experiments and Effect of pH

Loading experiments were carried out to investigate the effect of initial concentration on sorption. R_d values of Cs^+ and Ba^{2+} sorption on INaA at different initial cation concentrations and temperatures are given in Table 3 and Table 4, respectively.

The tables show that as the initial concentration increases, the R_d values decrease. This stems from the fact that as the initial concentration of the sorbate cation is

Table 3 The distribution ratio, ln R_d (ml/g), values of Cs^+ sorption onto INaA at different temperatures and initial concentrations, [C]° (mmol/ml)

		ln R_d values at different temperatures (K)			
Sorbent	[C]° (mmol/ml)	288	298	308	318
INaA	5×10^{-4}	6,11914	6,22862	6,00389	5,80513
	1×10^{-4}	8,42243	8,26722	7,94094	7,8917
	1×10^{-5}	9,19511	9,26427	9,27734	9,33891
5×10^{-6}	9,30424	9,33636	9,44074	9,42674	

Table 4 The distribution ratio, ln R_d (ml/g), values of Ba^{2+} sorption onto INaA at different temperatures and initial concentrations, [C]° (mmol/ml)

		ln R_d values at different temperatures (K)			
Sorbent	[C]° (mmol/ml)	298	308	318	328
INaA	1×10^{-4}	8,91547	9,02099	8,77017	8,83871
	1×10^{-5}	9,80171	10,04055	10,05589	–
	5×10^{-6}	10,17173	10,38492	10,18572	10,54944
1×10^{-6}	10,98316	10,20455	10,53175	10,67555	

increased, the ratio of the ions that are accommodated by the solid surface to those remaining in solution decreases, since a limited number of sites on the INaA are available for sorption.

The loading curves were constructed by plotting log R_d values against log $[C]_s$, at four different temperatures, in Figs. 7 and 8 for cesium and barium ion sorptions, respectively.

According to those curves, Cs^+ and Ba^{2+} sorption show similar shapes indicating that the sorption occurs on single sorption site between 5×10^{-4} and 1×10^{-6} concentration ranges. This sorption site is negatively charged oxygen atoms belonging to carboxylate and phenolate groups on INaA.

The increase of pH value has a substantial effect upon sorption of Ba^{2+} onto INaA, as shown in Fig. 9. It is seen that there is almost no adsorption between pH (1–2) range. In literature [7, 10] it is also emphasized that in aqueous media there is a competition between H_3O^+ and metal ions toward the solid phase, at low pH value, the surface of the adsorbent is closely associated with the hydronium ions and repulsive forces limit the approach of the metal ions. As we increase the pH value, we observe a dramatical increase at the uptake of Ba^{2+} by sorbent, due to the fact that principal adsorption sites -COOH and -COH dissociated to their anionic form -COO^- and -CO^-. This dissociation caused a negatively charged surface and cations

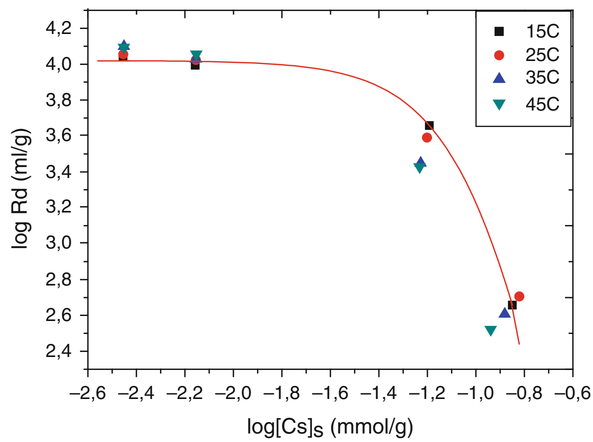

Fig. 7 The loading curves for sorption of Cs^+ onto INaA at different temperatures

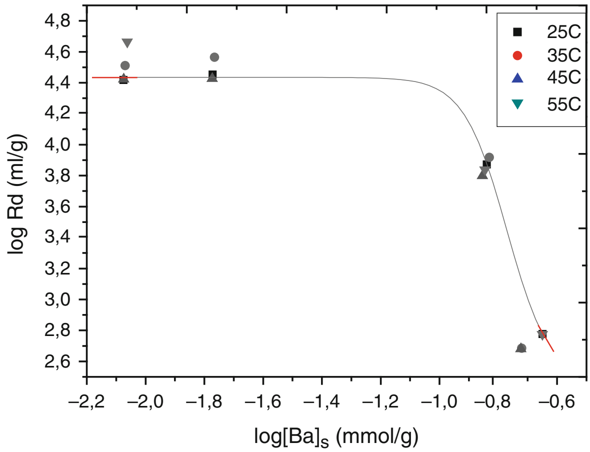

Fig. 8 The loading curves for sorption of Ba^{2+} onto NaIA at different temperatures

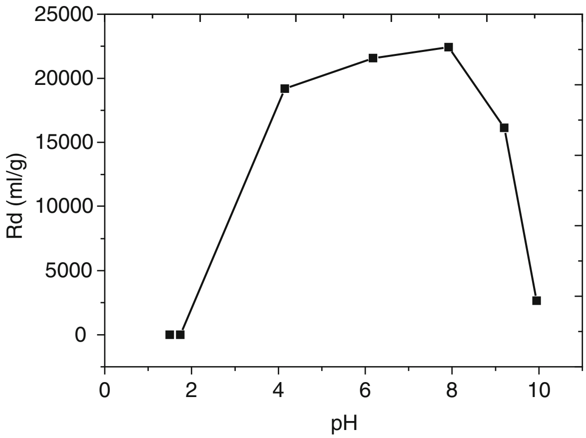

Fig. 9 Effect of pH upon sorption of Ba^{2+} onto INaA

could more easily adsorbed to solid surface. When pH value passes 8, we observe a sharp decrease at sorption capacity of sorbent, because INaA starts to dissolve and binded Ba^{2+} passes from solid phase to solution phase. As a result adsorption capacity of sorbent (INaA) increases with increasing pH as long as INaA doesn't dissolve in liquid phase.

4.5 Freundlich Isotherm

The isotherm plots for two cations at different loadings and temperatures on INaA are given in Figs. 10 and 11.

The freundlich constants n and k obtained for different sorption cases are given in Tables 5 and 6.

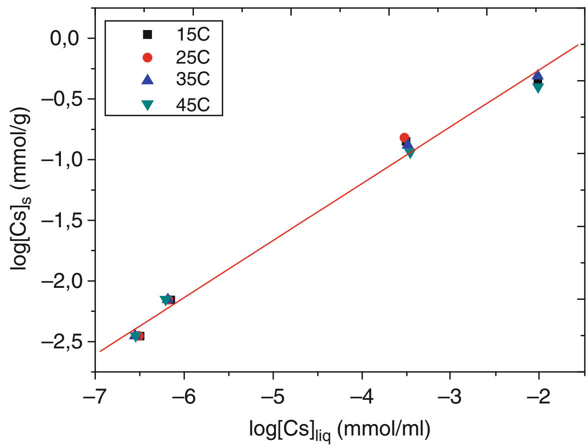

Fig. 10 Freundlich isotherm plots for sorption of Cs^+ onto INaA at various temperatures

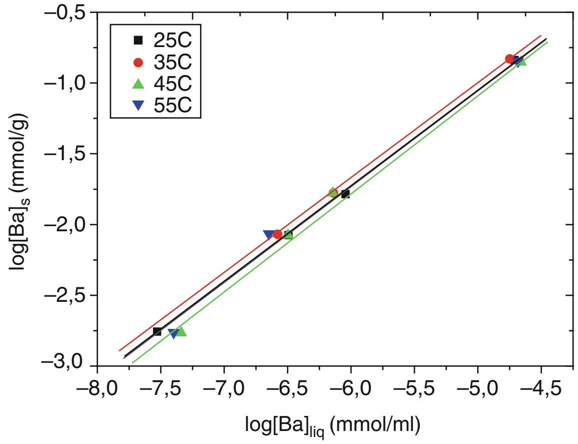

Fig. 11 Freundlich isotherm plots for sorption of Ba^{2+} onto INaA at various temperatures

Table 5 Freundlich constants, *n* and *k*, obtained from the least square fits of the sorption data of Cs^+ onto INaA (The linear correlation coefficients were all greater than 0.9905)

		Temperature (K)			
Sorbed cation	Freu. constant	288	298	308	318
Cs^+	*n*	0,4706	0,5305	0,4687	0,4455
	k	4,864	11,405	4,898	3,511

The values of n being less than 1.0 in all cases indicate a non-linear sorption that takes place on a heterogeneous surface. The non-linearity represents that the sorption energy barrier increases exponentially as the fraction of filled sites on sorbent increases. When we compare n values of Cs^+ and Ba^{2+} ions sorption on sorbent, it's

Table 6 Freundlich constants, *n* and *k*, obtained from the least square fits of the sorption data of Ba^{2+} onto INaA (The linear correlation coefficients were all greater than 0.9908)

		Temperature (K)			
Sorbed cation	Freu. constant	298	308	318	328
Ba^{2+}	*n*	0,6814	0,6777	0,7069	0,6891
	k	226,93	243,61	307,26	257,57

obvious that non-linear sorption behavior of Cs^+ is more than Ba^{2+}, this is one of the reason which explains lower R_d values of Cs^+ sorption.

The magnitude of k is proportional to sorption affinity. The significant difference between k values for the sorption behavior of two ions show that sorbent has a much higher tendency to adsorb barium ions when compared with cesium ions. It can be explained by charge. An increase in the oxidation state favors the accumulation of the ion on the sorption surface leading to electrostatic stability.

Increase of temperature has no pronounced effect on *n* values, but the *k* values in case of Ba^{2+} sorption has an increasing trend and for Cs^+ sorption, it has a decreasing trend, but the changes are not significant.

4.6 Dubinin-Radushkevich (D-R) Isotherms

The sorption datas of Cs^+ and Ba^{2+} fitted the D-R model well as shown in Figs. 12 and 13. The corresponding values of C_m, K and E are given in Tables 7 and 8.

C_m values indicate that barium ions are sorbed 5 times more than Cs^+ ions and decrease with increasing temperature, but changes are not significant. In all cases,

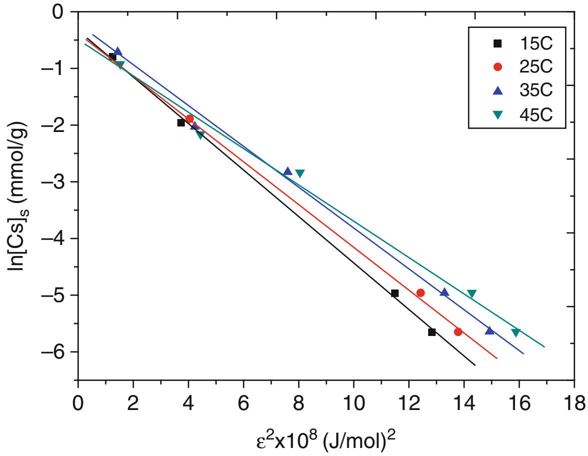

Fig. 12 Dubinin-raduskevich isotherm plots for sorption of Cs^+ onto INaA at various temperatures

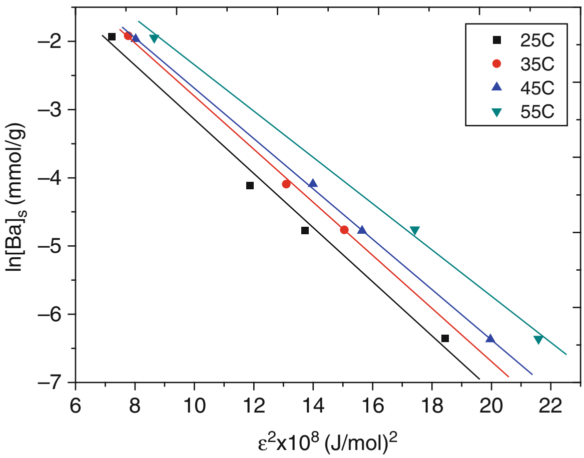

Fig. 13 Dubinin-raduskevich isotherm plots for sorption of Ba^{2+} onto INaA at various temperatures

Table 7 The D-R ısotherm constants, K (mol/kJ)^2, C_m (mmol/100 g), and E (kJ/mol) obtained from the least square fits for the sorption data of Cs^+ onto INaA. (The linear correlation coefficients were all greater than 0.9915)

		Temperature (K)			
Sorbed ion	D-R constant	288	298	308	318
Cs^+	C_m	71.1	71.1	74.4	60.0
	K	4.096×10^{-3}	3.793×10^{-3}	3.542×10^{-3}	3.162×10^{-3}
E	11,048	11,481	11,881	12,575	

Table 8 The D-R isotherm constants, K (mol/kJ)^2, C_m (mmol/100 g), and E (kJ/mol) obtained from the least square fits for the sorption data of Ba^{2+} onto INaA. (The linear correlation coefficients were all greater than 0.9973)

		Temperature (K)			
Sorbed ion	D-R constant	298	308	318	328
Ba^{2+}	C_m	349.2	310.0	276.4	276.1
	K	4.439×10^{-3}	3.945×10^{-3}	3.690×10^{-3}	3.380×10^{-3}
E	10,613	11,258	11,641	12,163	

the mean free energy of sorption, E, is in 8–16 kJ/mol energy range corresponding to ion-exchange type of sorption [22]

4.7 *Thermodynamic Results*

The values of $\Delta H°$ and $\Delta S°$ of Cs^+ and Ba^{2+} sorption were obtained by fitting the experimental data to Arrhenius equations (11) and (12) given below. The results are shown in Figs. 14 and 15.

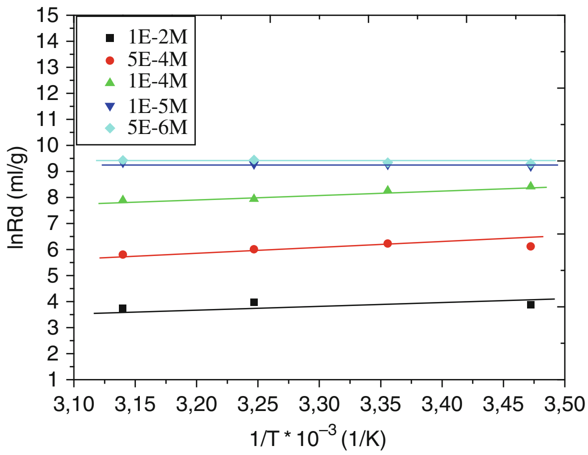

Fig. 14 Arrhenius plots for sorption of Cs^{+} onto INaA

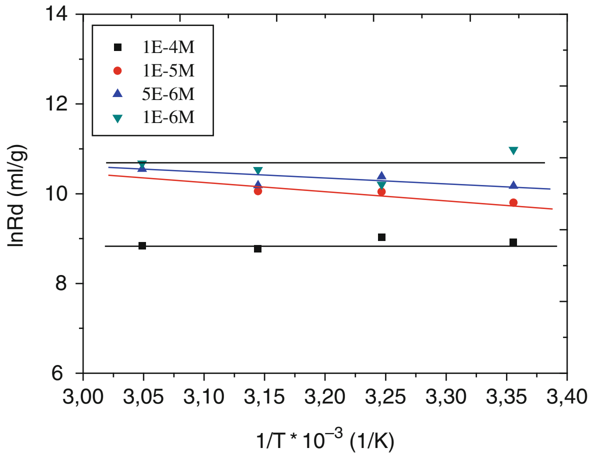

Fig. 15 Arrhenius plots for sorption of Ba^{2+} onto INaA

$$\ln\ R_{\mathrm{d}} = \frac{\Delta S^{\circ}}{R} - \frac{\Delta H^{\circ}}{RT} \tag{11a}$$

$$\Delta G^{\circ} = \Delta H^{\circ} - T\Delta S^{\circ} \tag{12a}$$

The results are given in Tables 9 and 10 and Figs. 14 and 15.

Enthalpy changes show the dependence of sorption processes to the temperature. When we examine the ΔH° values for Cs^{+} and Ba^{2+} sorption onto INaA, it is clear that those processes are not significantly affected by the temperature change, because ΔH° values are quite close to zero. However, sorption behavior of Cs^{+} onto INaA is an exothermic, and for Ba^{2+}, it is an endothermic process. In liquid-solid

Table 9 The average values of the enthalpy change, ΔH°_{av} (kJ/mol), entropy change, ΔS°_{av} (J/mol.K) and the calculated values of the Gibbs free energy change, ΔG° (kJ/mol), obtained at different temperatures for the sorption case of Cs^+ onto INaA

			ΔG° (kJ/mol) at different temperatures (K)			
Sorbed ion	ΔH°_{av} (kJ/mol)	ΔS°_{av} (J/mol.K)	288	298	308	318
Cs^+	−3.673	48.85	−17.74	−18.23	−18.72	−19.21

Table 10 The average values of the enthalpy change, ΔH°_{av} (kJ/mol), entropy change, ΔS°_{av} (J/mol.K) and the calculated values of the Gibbs free energy change, ΔG° (kJ/mol), obtained at different temperatures for the sorption case of Ba^{2+} onto INaA

			ΔG° (kJ/mol) at different temperatures (K)			
Sorbed ion	ΔH°_{av} (kJ/mol)	ΔS°_{av} (J/mol.K)	298	308	318	328
Ba^{2+}	2.102	89.522	−24.575	−25.470	−26.366	−27.261

systems, when temperature is increased, the behavior of ions in solution or on the solid will subject to factors such as the interionic forces, the hydration energy, the availability of sorption sites and the relative stability of sorbed ions at these sites [23]. Exothermic behavior of Cs^+ ion sorption onto INaA can be explained by the thermal destabilization leading to an increase of the mobility of cesium ions on the surface of the solid as the operating temperature is increased, thus enhancing the desorption steps, that is, increasing thermal energy of ions do not favor to be bound of ions to the surface. Positive ΔH° value for Ba^{2+} sorption and therefore, we should think of the differences which makes more the difficult the uptake of Ba^{2+} ions onto INaA. There is a large difference in hydration enthalpies [24], being −276 kj/mol for Cs^+ and −1,305 kj/mol for Ba^{2+} ions. In literature [25] it is reported that metal ions with high hydration energies are well solvated in water and for cations that are solvated well in water, sorption requires that such ions should be stripped out to a certain extent of their hydration shell which is a process that requires energy input. If this dehydration energy exceeds the exothermicity associated with the sorption of a metal ion on a solid, then the overall energy balance will lead to an endothermic behavior.

ΔH° values for Cs^+ and Ba^{2+} sorption onto INaA indicate the physical nature of the sorption process which correspond to weak electrostatic attractions. Sorption behavior of Cs^+ onto INaA is an exothermic, and for Ba^{2+}, it is an endothermic process.

In all cases, positive ΔS° values were obtained upon Cs^+ and Ba^{2+} sorption. Positive ΔS° values are usually associated with a spontaneuos process where the system shows an endothermic behavior or even a weak exothermic behavior and also it can be said that more disorder is generated in the system upon sorption.

As the exothermic behavior becomes more pronounced negative ΔS° values are obtained [26].

It was also found in Tables 9 and 10 that, ΔS° value of Ba^{2+} sorption onto INaA is approximately two times more than Cs^+. In literature, it's reported that the positive values of ΔS° resulting from sorption of divalent cations (Ba^{2+} in this case) on solid surfaces might suggest that ions displaced from the solid surface are greater in number than the sorbed Ba^{2+} ions, which means that two monovalent ions (Na^+ in this case) may be exchanged for a single Ba^{2+} ion [27, 26].

The calculated negative values of ΔG° for all cases indicate that the sorption process of each is spontaneous and preferentially driven toward the products. Temperature change has no significant effect on ΔG° values for both sorptions.

References

1. Shahwan T, Erten HN (2002) Thermodynamic parameters of CS+ sorption on natural clays. J Radioanal Nucl Chem 253(1):115–120
2. Ebner AD, Ritter JA, Navratil JD (2001) Adsorption of Cesium, strontium and cobalt cons of Magnetite and magnetile-silica composite. Ind Eng Chem Res 40:1615–1623
3. Shahwan T, Erten HN (2004) Temperature effects in Barium Sorption on Natural Kaolinite and Chlorite-Illite Clays. J Radioanal Nucl Chem 260:1, 43–48
4. Diallo MS, Simpson A, Gassman P, Faulon JL, Johnson Jr JH, Goddard WA III, Hatcher PG (2003) 3-D structural modeling of humic acids through experimental characterization, computer assisted structure elucidation and atomistic simulations. Environ Sci Technol 37:1783–1793
5. Steelink C (2002) Investigating Humic Acids in soils. Anal Chem A-Pages 74:326A–333A
6. Sutton R, Sposito G (2005) Environ Sci Technol 39:9009–9015
7. Gezici O, Kara H, Ersöz M, Abali Y (2005) The sorption behavior of Nickel immobilized Humic Acid System in a Column arrangement. J Colloid Interface Sci 292:381–391
8. Seki H, Suzuki A (1995) Adsorption of Heavy metals ontu insolubilized Humic Acid. J Colloid Interface Sci 171:490–494
9. Azizian S (2004) Kinetic models of sorption: a theoretical analysis. J Colloid Interface Sci 276:47–52
10. Baker H, Khalili F (2004) Analysis of the removal of lead (II) from aqueous solution by adsorption onto insolubilized humic acid: Temperature and pH dependence. Anal Chim Acta 516:179–186
11. El-eswed B, Khalili F (2006) Adsorption of Cu (II) and Ni (II) on solid humic acid from the Azrageria Jordan. J Colloid Interface Sci 299:497–503
12. Shahwan T, Suzer S, Erten HN (1998) Sorption studies of CS+ and Ba 2+ cations on magnasite. Appl Radiat Isot 49:8, 915–921
13. Tinsley IJ (2004), Chemical concepts in pollutant behavior, Wiley-Interscience, New York
14. Masini JC, Abate G, Lima EC, Hahn LC, Nakamura MS, Lichtig J, Nagatomy HR (1998) Comparison of methodologies for determination of carboxylic and phenolic groups in humic acids. Anal Chim Acta 364:223–233
15. Gran G (1952) Determination of Equivalence Point in Polentiomertic titrations. Analyst 77:661
16. Benites VM, Mendonca E, Schaefer CEGR, Novotny EH, Reis EL, Ker JC (2005) Properties of black soil humic acids from high altitude rocky compleves in Brazil. Geoderma 127:104–113
17. Shirshova LT, Ghabbour EA, Davies G (2006) Spectrosegnic characterization of humic acid fractions isolated from soil using different extraction procedures. Geoderma 133:204–216

18. Xu D, Zhu S, Chen H, Li F (2006) Non-covalent association between hydrophobic organic contaminants and dissolved organic material observed by NMR. Colloids Surf A Physicochem Eng Aps 276:1–7
19. Simpson MJ, Simpson AJ, Hatcher PG (2004) Structural characterization of a Fulvic acid and a Humic acid using Solid-state Ramp-CP-MAS 13 CNMR. Environ Toxicol Chem 23(2):355–362
20. Cook RL, Langford C (1998) Structural differences between humic fraction from different soil types as determined by FT-IR and 13 C-NMR. Environ Sci Technol 32:719–725
21. Frund R, Ludemann HD, Gonzalez-Vila FJ, Almendros G, del Rio JC, Martin F (1989) Structural differences between humic fraction from different soil types as determined by FT-IR and 13 C-NMR. Sci Total Environ 81/82:187–194
22. Helferrich F (1964) Ion exchange. Mc Graw Hill, New York
23. Shahwan T, Erten HN, Unugur S (2006) A characterization study of some aspect of the adsorption of aqueous Co (2+) ions on a natural bentonite. J Colloid Interface Sci 300:447–452
24. http://www.science.uwaterloo.ca/?cchieh/cact/applychem/hydration.html
25. Akar D, Shahwan T, Eroglu AE (2005) Kinetic and thermodynamic investigation of Strontium ions Retention by natural kaolnite and chlinoptilite Minerals. Radiochimica Acta 93:477–485
26. Khan SA, Reman RU, Khan MA (1995) Adsorption of CS (I), Sr (II) and Co (II) on Al2 O3. J Radioanal Nucl Chem 190:81
27. Shahwan T (2000) Ph.D Thesis, Department of Chemistry, Bilkent University, Ankara, Turkey